Journal of Molecular Catalysis B: Enzymatic 76 (2012) 9–14

Contents lists available at SciVerse ScienceDirect

Journal of Molecular Catalysis B: Enzymatic

journal homepage: www.elsevier.com/locate/molcatb

Nanoparticle-supported consecutive reactions catalyzed by alkyl hydroperoxide reductase

Liang Wang, Yuan Chen, Rongrong Jiang*

School of Chemical & Biomedical Engineering, Nanyang Technological University, 62 Nanyang Drive, Singapore 637459, Singapore

ARTICLE INFO

Article history:
Received 24 February 2011
Received in revised form
25 November 2011
Accepted 25 November 2011
Available online 16 December 2011

Keywords:
Alkyl hydroperoxide reductase
Single-walled carbon nanotubes
Multi-enzyme immobilization

ABSTRACT

Multi-enzyme systems have been widely employed in biotransformations to produce a variety of useful compounds. An efficient and stable multi-enzyme system is often required for large-scale applications. Herein we report the immobilization of a multi-enzyme system, which catalyzes consecutive reactions by alkyl hydroperoxides reductase (AhpR) on functionalized single-walled carbon nanotubes (SWCNTs). AhpR, composed of H_2O_2-forming NADH oxidase (nox) and peroxidase (AhpC), protects microorganisms from the toxic effects caused by organic hydroperoxides and regulates H_2O_2-mediated signal transduction. Both His-tagged nox and AhpC were immobilized via non-covalent specific interactions between His-tagged proteins and modified SWCNTs. The activity and stability of AhpR at different nox/AhpC ratios were examined and the immobilized AhpR system demonstrated ca. 87% of the native enzyme activity. We found that various nox/AhpC ratios may affect overall AhpR activity but not the total turnover number. The amount of intermediate hydrogen peroxide is not influenced by immobilization and it decreases when the weight of AhpC increases, and becomes undetectable when nox/AhpC ratio reaches above 1:50. Hence, we believe that this non-covalent specific immobilization procedure can be applied to multi-enzyme systems with satisfactory activity retention and stability improvement during consecutive reactions.

1. Introduction

Biotransformations often involve multi-enzyme systems that carry out serial reactions to yield diverse products such as alcohols, amines, and enantiomerically pure compounds [1–4]. An efficient and clean multi-enzyme system can be used in multi-step complex synthetic routes via isolated biocatalysts in vitro, such as the bioproduction of methanol from CO_2 by co-immobilizing three enzymes on protamine-templated titania [5], and the conversion of L-asparagine to glutamate via attaching L-asparaginase and glutamate dehydrogenase on agarose beads [6].

As compared to whole-cell system, cell-free multi-enzyme system has several advantages [7,8]: (i) reduced complexity and easy reaction control, including optimization of biocatalyst and substrate concentrations, change of reaction media, and variation of different enzyme ratios; (ii) unnecessary to consider substrate toxicity to the system; (iii) the high purity of final products due to the absence of side-reactions and metabolite contamination. However, the relatively low stability of isolated biocatalysts is one of the general technical hurdles that hamper large-scale applications [9,10].

Enzyme immobilization allows biocatalysts to have improved stability in both aqueous and organic phases, circumvent the contamination from final products and easy recovery from reaction medium [11–13]. Specifically, multi-enzyme immobilization system has been applied as biosensor to detect O_2 [14], L-malate [15], and glucose [16,17]. Some chemical manufacturing routes derived from metabolic pathways have also been engaged in multi-enzyme immobilization systems, such as the production of methanol, ethanol, and L-lactic acid [18,19].

In recent years, enzyme immobilization with nanoscale supporting materials has attracted much attention in biocatalysis as these nanomaterials could provide high surface area and reduce mass-transfer resistance [20–22]. Compared to the studies on mono-enzyme immobilization, research of multi-enzyme system immobilization on nanostructures is considerably less. For mono-enzyme immobilization, commonly used immobilization approaches, such as adsorption, entrapment and covalent binding, often cause enzyme leaching [23], enzyme 3D structure change [24], and mass-transfer resistance [25]. Our group has previously demonstrated an efficient mono-enzyme immobilization method based on the non-covalent specific interaction between His-tagged enzyme and N_α, N_α-bis(carboxymethyl)-L-lysine hydrate (ANTA) functionalized nanostructures, which overcomes the foresaid limitations[26–28]. Other nanoparticles have also been used in protein attachment based on the polyhistidine–Co^{2+}/Ni^{2+}

* Corresponding author. Tel.: +65 65141055; fax: +65 67947553.
E-mail address: rrjiang@ntu.edu.sg (R. Jiang).

1381-1177/$ – see front matter © 2011 Elsevier B.V. All rights reserved.
doi:10.1016/j.molcatb.2011.11.016

interaction [29–33], but most are for biosensing or detecting purposes. As for multi-enzyme system immobilization, other factors such as the ratios between different enzymes, overall activity and stability, and intermediate formation also need to be considered.

In this work, we apply the aforementioned non-covalent specific immobilization approach on a multi-enzyme system that carries out consecutive reactions with supporting materials single-walled carbon nanotubes (SWCNTs). Alkyl hydroperoxide reductase (AhpR), which has been found in many anaerobic bacteria such as *Salmonella typhimurium* (*S. typhimurium*) [34], *Streptococcus mutans* [35], *Amphibacillus xylanus* [36], and *Lactococcus lactis* [37], can protect microorganisms from the toxic effects caused by organic hydroperoxides. Moreover, it was found to regulate hydrogen peroxide-mediated signal transduction in eukaryotes [38]. It is composed of two enzymes – H_2O_2-forming NADH oxidase (nox, encoded by *ahpF*) and peroxidase (encoded by *ahpC*) [39]. Since the overall reaction of AhpR, as shown in the following, is identical to the water-forming NADH oxidase where oxygen is the substrate [40,41], AhpR can also serve to regenerate NAD^+ in oxidoreductive reactions that requires nicotinamide cofactors [37,42].

$$\text{Nox}: \quad O_2 + \text{NADH} + H^+ \rightarrow NAD^+ + H_2O_2$$

$$\text{Peroxidase(AhpC)}: \quad H_2O_2 + \text{NADH} + H^+ \rightarrow NAD^+ + 2H_2O$$

$$\text{Overall}: \quad O_2 + 2\text{NADH} + 2H^+ \rightarrow 2NAD^+ + 2H_2O$$

Previous work on AhpR (*S. typhimurium*) has demonstrated that AhpC has no activity when nox is absent [43] – AhpC requires electron transport from the N-terminal disulfide bond of nox to the inter-subunit disulfide bond between AhpC and nox within temporal interaction [36] (Fig. 1). The collision between the two immobilized enzymes is expected to enable desired consecutive reactions. Here in this work, we aim to demonstrate that the specific non-covalent interaction based immobilization approach (polyhistidine-Co^{2+}) is also suitable for multi-enzyme immobilization to catalyze consecutive reactions. Even for a coupled enzyme system, enzyme activity can be well maintained after immobilization via this method. Our model system is the annotated AhpR from *Bacillus cereus* (*B. cereus*), which shares high amino acid level identity (>55%) with AhpR from *S. typhimurium*. The activity and stability of AhpR, nox/AhpC ratios, and the intermediate hydrogen peroxide generated during catalysis have been investigated in this study.

2. Materials and methods

2.1. Materials

Bradford reagent, ampicillin, kanamycin, potassium phosphate, sodium chloride, tryptone, cobalt chloride, nitric acid, sulfuric acid, 5-bromo-4-chloro-3-indolyl-beta-D-galactopyranoside (X-Gal), N_α,N_α-bis(carboxymethyl)-L-lysine hydrate (ANTA), 1-ethyl-3-[3′-(dimethylamino)propyl]carbodiimide (EDC), *N*-hydroxysuccinimide (NHS), N-(2-hydroxyethyl) piperazine-N′-(2-ethanesulfonic acid) (HEPES), and isopropyl β-D-1-thiogalactopyranoside (IPTG) were purchased from Sigma–Aldrich. Dithiothreitol (DTT), β-nicotinamide adenine dinucleotide, reduced dipotassium salt (NADH), and flavin adenine dinucleotide (FAD) were obtained from Merck. Low melting agarose was obtained from Nusieve. *Taq* DNA polymerase and T4 DNA ligase were from New England Biolabs. Restriction endonucleases *Bgl*II and *Xho*I were purchased from Fermentas. Super purified HiPco® Single-walled carbon nanotubes were purchased from Unidym (USA, *D*: 0.8–1.2 nm, length: 100–1000 nm, surface area per unit mass: 1315 m^2/g).

2.2. AhpC cloning, overexpression and protein purification

The *ahpC* gene from *B. cereus* ATCC 14579 was amplified by polymerase chain reaction (PCR) using *Taq* DNA polymerase with primers 5′-AGATCTGACCATGGCGATGTTATTAATCGGCACAGAAGTAA-3′ and 5′-CTCGAGGGATCCCTATTAGATTTTGCCTACAAGGTCAAG-3′. The PCR products were purified by gel extraction kit (QIAGEN) and cloned into pDrive vector with blue/white screening features (PCR cloning kit, QIAGEN). Recombinant plasmid pDrive-*ahpC* was obtained by miniprep (QIASpin Miniprep kit, QIAGEN), and checked with DNA sequencing. The plasmid was then digested by restriction endonucleases *Bgl*II and *Xho*I, cloned into pET-30b (+) (Novagen) to obtain recombinant plasmid pET30b-*ahpC*, and transferred into *E. coli* BL21 (DE3) competent cells (Stratagene). AhpC was overexpressed at 37 °C with 200 μM IPTG induction when the absorbance reached 0.6–0.8 at 600 nm. After 3-h overexpression, cell pellet was collected by centrifugation and lysed in 50 mM, pH 7.0 HEPES buffer through sonication at 30 s × 8 with 30 s intervals. AhpC was purified by immobilized metal affinity chromatography using Gravatrap Ni^{2+} column (GE Healthcare) and desalted by PD-10 column (GE Healthcare) according to manufacturer's instructions. The purity of AhpC was verified by sodium dodecyl sulfate polyacrylamide gel electrophoresis (SDS-PAGE) and AhpC concentration was measured after 5-min incubation with Bradford Reagent using Biophotometer (Eppendorf).

2.3. SWCNTs modification

SWCNTs were first treated with HNO_3/H_2SO_4 mixture (HNO_3/H_2SO_4 = 1:3) to form SWCNT–COOH, then activated by NHS/EDC in 20 mM, pH 7.5 HEPES buffer to convert SWCNT–COOH to SWCNT–NHS ester complex, and finally the ester complex reacted with ANTA–Co^{2+} to produce SWCNT–ANTA–Co^{2+} complex according to a previously reported protocol [26]. SWCNTs modification was verified by Fourier transform inferred spectroscopy. Functionalized SWCNT samples were filtered with 0.2-μM nylon membrane and washed by distilled water for three times.

2.4. Enzyme immobilization

Cell lysis was carried out in 20 mM, pH 7.5 HEPES buffer by sonication (30 s × 8) and centrifuged at 30, 000 × g for 30 min. The supernatant was incubated with SWCNT–ANTA–Co^{2+} complex at 4 °C overnight. SWCNT–ANTA–Co^{2+}–AhpC conjugate (SWCNT–AhpC) was purified and washed with 20 mM, pH 7.5 HEPES buffer containing 20 mM imidazole three times. SWCNT–AhpC was suspended in 20 mM, pH 7.5 HEPES buffer.

2.5. Circular dichroism

The secondary structure of free AhpC and SWCNT–AhpC was detected by circular dichroism spectroscopy (CD). CD measurement was carried out by a ChiraScan circular dichroism spectrometer (Applied Photophysics, United Kingdom) with constant N_2 flushing. The far-UV CD spectra (200–260 nm) were obtained in 10 mM, pH 7.0 potassium phosphate buffer containing ~0.34 mg/ml enzyme in a 1-mm path length quartz cuvette at room temperature. Each spectrum is obtained from the average reading of three consecutive scans. The contents of α-helix and β-sheet were calculated based on the mean residue ellipticity at 222 and 218 nm. The spectrum of pristine SWCNTs was also acquired under the same conditions.

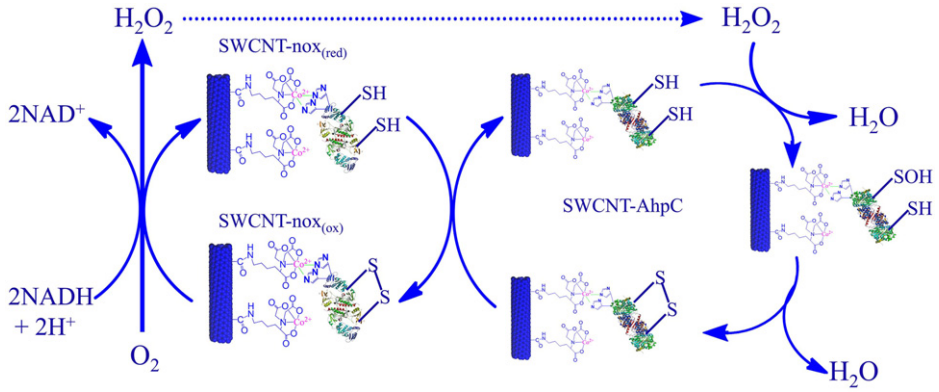

Fig. 1. Proposed scheme of consecutive reactions catalyzed by immobilized AhpR. SWCNT-nox initially obtains electrons from NADH via the flavin and dithiol–disulfide interchange, while reducing oxygen to intermediate hydrogen peroxide. Electrons are then transferred from the active site of nox to the dithiol center of AhpC followed by the reduction of hydrogen peroxide to final product water. Since AhpC requires electrons from nox, it cannot catalyze the reductive reaction by itself [35,43].

2.6. AhpR activity with different nox/AhpC ratio

The activity of free and immobilized AhpR system was measured by tracking NADH absorbance decrease at 340 nm (ε: 6220 $M^{-1}cm^{-1}$) with a DU 800 spectrophotometer (Beckman Coulter, USA). Standard conditions include air-saturated 50 mM, pH 7.0 potassium phosphate buffer (PPB) containing 200 μM NADH and 8 μM FAD (free nox)/23.95 μM FAD (SWCNT-nox) at 30 °C. Four combinations of AhpR system (nox/AhpC, SWCNT-nox/AhpC, nox/SWCNT-AhpC, and SWCNT-nox/SWCNT-AhpC) with different nox/AhpC molar ratios (100: 1, 10: 1, 1: 1, 1:10, 1: 30, and 1: 50) were tested under standard conditions. In this study, the activity of free nox is assigned to 100%. "Relative activity" is defined as the activity of AhpR system over the activity of equal amount of free nox.

2.7. Enzyme stability measurement

2.7.1. Storage stability

Storage stability was examined at 4 °C and 20 °C over a period of 1000 h. Activity was measured under standard conditions with nox/AhpC at 1:1.

2.7.2. Total turnover number

Free nox, SWCNT-nox, and four combinations of AhpR system with different nox/AhpC ratios (100: 1, 10: 1, 1: 1, 1:10, and 1:30) were added into the air-saturated 50 mM, pH 7.0 PPB buffer with/without 5 mM DTT at 30 °C. NADH was added until nox or AhpR could no longer catalyze the reaction [42].

2.8. Amplex red assay

The oxidation of 9-acetylresorufin (Amplex Red, Molecular Probe, Invitrogen, Singapore) catalyzed by horseradish peroxidase (HRP) was used to detect H_2O_2 quantitatively. The reaction is carried out according to a strict 1:1 stoichiometry between H_2O_2 and Amplex Red, and generates the fluorescent product resorufin (ε: 54, 000 $M^{-1}cm^{-1}$, excitation: 530 nm, and emission: 590 nm). Samples from free nox, SWCNT-nox, and the four combinations with different nox/AhpC ratios (100: 1, 10: 1, 1: 1, 1: 10, 1: 30, and 1: 50) were pipetted into a 96-well microplate after reacting with 200 μM NADH under standard conditions, respectively. The working solution (50 μl) containing Amplex Red reagent and HRP was added to the 96-well microplate subsequently and the reaction lasted for 30 min in dark at room temperature. The fluorescence of resorufin was detected by a microplate reader at 590 nm (Tecan Infinite® 200 Pro, SciMed, Singapore).

3. Results and discussion

3.1. Cloning, overexpression and purification of AhpC

The *ahpC* gene has been successfully amplified by PCR with genomic DNA from *B. cereus* as template. The nucleotide sequence of *ahpC* was confirmed by DNA sequencing, showing one silent mutation (GAA to GAG) at position Glu164 compared to the annotated gene sequence from NCBI. The overexpressed AhpC reveals a prominent band on SDS-PAGE (Fig. 2 lane C). The open reading frame of *ahpC* encodes the enzyme with a molecular weight of ~25 kDa, which is in agreement with the SDS-PAGE result that exhibits only one band at the right size after immobilized metal affinity chromatography purification (Fig. 2 lane F).

3.2. SWCNT–AhpC

We modified the surface of SWCNTs to enable the specific attachment of His-tagged enzyme AhpC. The pristine SWCNTs were first treated with acid mixture in the presence of NHS/EDC, and then functionalized with nitrilotriacetate group terminated with Co^{2+} as reported previously [26]. The resulting SWCNT–ANTA–Co^{2+} complex was incubated with cell lysate containing His-tagged AhpC overnight to obtain SWCNT–AhpC conjugate. We confirmed the binding specificity of AhpC to SWCNT–ANTA–Co^{2+} complex by eluting the enzyme off the conjugate with imidazole and checked with SDS-PAGE. The SDS-PAGE exhibits only one band (~25 kDa) after elution (Fig. 2 lane I), and no band is shown for the control (SWCNT–COOH and AhpC mixture) (Fig. 2 lane H). The

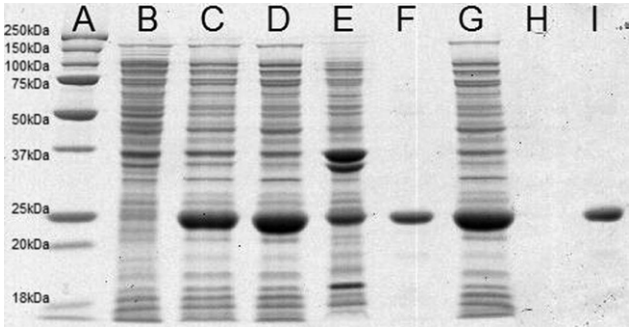

Fig. 2. SDS-PAGE of AhpC overexpression, purification and immobilization. Lane A: protein weight marker; lane B: uninduced cells; lane C: induction with IPTG; lane D: cell lysate; lane E: insoluble part; lane F: purified AhpC; lane G: cell lysate; lane H: imidazole elution sample from control (SWCNT–COOH and AhpC mixture); Lane I: imidazole elution sample from SWCNT–AhpC.

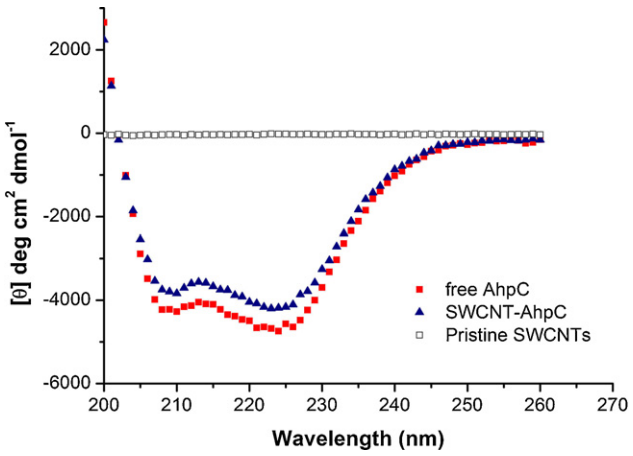

Fig. 3. Circular dichroism spectra of free AhpC (■, SWCNT-AhpC (▲), and modified SWCNTs (□).

amount of AhpC in cell lysate also decreased after immobilization, which suggests successful enzyme immobilization (data not shown here). These results indicate that His-tagged AhpC can attached to SWCNT–ANTA–Co^{2+} complex specifically. In order to determine the loading capacity of AhpC, we investigated three different AhpC to SWCNTs ratios (w/w), 5:1, 10:1, and 15:1. The immobilization capacity was found to be ~0.78 mg enzyme/mg SWCNTs at all ratios tested.

3.3. Circular dichroism

In order to examine the secondary structure of AhpC after immobilization, we used CD spectroscopy. Fig. 3 demonstrates the CD spectra of free AhpC, SWCNT–AhpC, and modified SWCNTs in the far-UV region. The mean residue ellipticity at 222 nm and 218 nm is used to quantify α-helix and β-sheet contents. As shown in Table 1, the α-helix or β-sheet content of SWCNT–AhpC is very similar to that of native AhpC, reflecting that the supporting materials SWCNTs do not affect the AhpC structure significantly. The preservation of enzyme conformation may be attributed to the specific interaction between the His-tagged enzyme and SWCNT–ANTA–Co^{2+} complex.

3.4. AhpR activity with different nox/AhpC ratios

Activity retention is one of most important features to evaluate the performance of immobilized enzyme. The AhpR activity of four different combinations (nox/AhpC, nox/SWCNT–AhpC, SWCNT–nox/AhpC, and SWCNT–nox/SWCNT–AhpC) has been investigated at various nox/AhpC ratios (Fig. 4). When nox/AhpC ratio is at 100:1 or 10:1, i.e., nox is in great excess of AhpC, the relative activity of all four combinations is close to 100%, which suggests that nox dominates the activity of AhpR system when the amount of AhpC is too little to make any difference. Moreover, the relative activity of all combinations was almost the same, which also suggests that the activity of SWCNT–nox is similar to that of free nox, consistent with our previous findings [26].

Table 1
α-Helix and β-sheet contents of free AhpC and SWCNT-AhpC.

Sample	α-helix (%)	β-sheet (%)
AhpC	30.6 ± 0.40	42.7 ± 0.75
SWCNT–AhpC	28.9 ± 0.91	41.6 ± 0.28

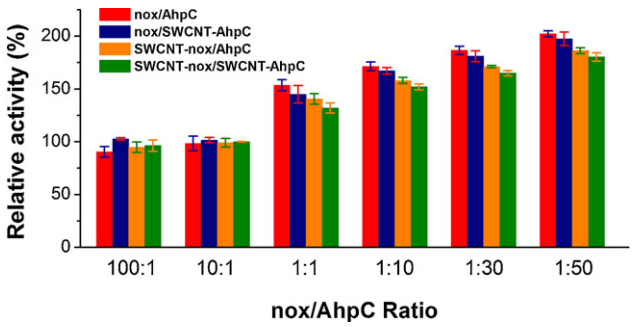

Fig. 4. Relative activity of both free and immobilized AhpR at various nox/AhpC ratios. nox/AhpC (red); nox/SWCNT–AhpC (blue); SWCNT-nox/AhpC (yellow) and SWCNT-nox/SWCNT–AhpC (green). (For interpretation of the references to color in this figure legend, the reader is referred to the web version of the article.)

The relative activity of all combinations increases from ~150% to ~200% as the nox/AhpC ratio increases from 1:1 to 1:50. The raise in AhpC leads to the increase of overall AhpR activity, which implies an increase in electron transfer rate from nox to AhpC and faster conversion of intermediate hydrogen peroxide to water (hydrogen peroxide data shown in Section 3.5) [34,43]. Free AhpR demonstrates the best activity among all four combinations. The decrease in AhpR activity of immobilized enzymes may be attributed to the steric hindrance caused by the supporting materials [6], which could have influenced the effective collisions between nox and AhpC. SWCNT–nox/SWCNT–AhpC system can still keep ~87% of free AhpR activity. The satisfactory activity retention may be attributed to the specific interaction between modified SWCNTs and His-tagged enzymes, which might help preserve enzyme structure during catalysis [33]. In addition, the similar mobility through Brownian motion between nanoparticle–immobilized enzymes and free enzymes could also help retain high activity [44,45].

3.5. Hydrogen peroxide formation

The intermediate, hydrogen peroxide, was determined by Amplex Red assay through monitoring resorufin fluorescence at 590 nm. As indicated by Fig. 5, supporting material SWCNTs do not influence the amount of hydrogen peroxide in all four combinations, which suggests that SWCNTs may not facilitate or block the electron transfer between nox and AhpC. With the same amount of NADH added, both free and SWCNT–nox produced

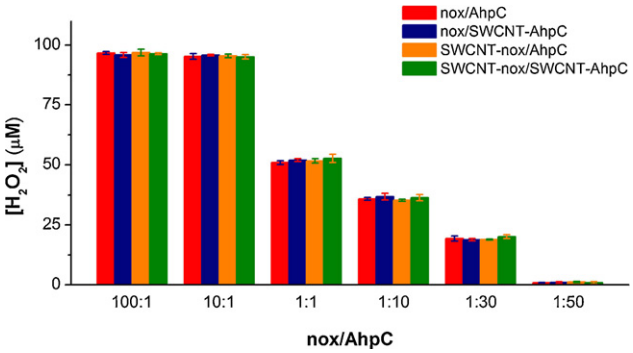

Fig. 5. Hydrogen peroxide generation from free and immobilized AhpR at different nox/AhpC ratios. nox/AhpC (red); nox/SWCNT–AhpC (blue); SWCNT–nox/AhpC (yellow); and SWCNT–nox/SWCNT–AhpC (green). (For interpretation of the references to color in this figure legend, the reader is referred to the web version of the article.)

similar amount of hydrogen peroxide, and that amount is close to previous findings on nox from other microorganisms [36,46]. In theory, AhpR is active as a one-molecule nox and one-molecule AhpC protein complex, and the reduction of intermediate hydrogen peroxide to water should be immediate and complete. Nevertheless, we found that when nox/AhpC is 1:1, half of the hydrogen peroxide still remains in the system when compared to free or immobilized nox. Hydrogen peroxide is only undetectable when nox/AhpC ratio reaches above 1:50. The incomplete turnover of hydrogen peroxide at lower nox/AhpC ratios may be owing to the unproductive collisions between nox and AhpC in reaction mixture [42]. Therefore, either free or immobilized AhpC has to be present in vast excess in order to be an effective H_2O_2 scavenger.

3.6. AhpR stability

Stability improvement is another key parameter to evaluate immobilized enzymes. We chose nox/AhpC ratio at 1:1, the theoretical ratio of AhpR protein complex, to study AhpR storage stability. Since the stability of SWCNT-nox has been investigated before [26], here we use SWCNT-AhpC and free nox as our AhpR system. As shown in Fig. 6, the storage stability of AhpR has been improved significantly compared to free AhpR at 4 °C and 20 °C. AhpR stored at 4 °C can still maintain >90% activity after ~1000 h, whereas free AhpR only keeps ca. 60% activity. The estimated half-life of SWCNT-AhpC at 20 °C is ~1200 h, twice that of free AhpC (~550 h). Factors such as high surface curvature [21], high loading capacity [47], and nanospatial confinement [20] may lead to the elevated enzyme stability after immobilization.

The operational stability of both free and immobilized AhpR system was investigated through their total turnover numbers (TTN). All combinations, including free nox/AhpC (Fig. 7a), SWCNT–nox/free AhpC (Fig. 7c), free nox/SWCNT–AhpC (Fig. 7b), and SWCNT–nox/SWCNT–AhpC (Fig. 7d) exhibit excellent operational stability with similar TTN at $\sim 9 \times 10^4$, indicating that immobilization has no influence on enzyme operational stability. Neither AhpC nor SWCNT–AhpC enhances the TTN of nox or SWCNT–nox, implying that the deactivation of AhpR is caused by the hydrogen peroxide produced by nox [42,48]. It was reported previously that the over-oxidation of the Cys at the nox active site, converting the original thiol group –SH to toxic sufinic acid–SOOH, may lead to enzyme inactivation [49]. Hence, the TTN is determined by the enzyme itself, and not influenced by immobilization. Despite adding exogenous DTT into the reaction system, the TTN of AhpR remains unchanged in all combinations. One possible explanation is that the second thiol of nox can behave as a stabilizing nucleophile at the active site. Therefore, the operational stability of AhpR is determined by the overoxidation of Cysteine residue at the active site of nox, and not by SWCNTs or AhpC [50].

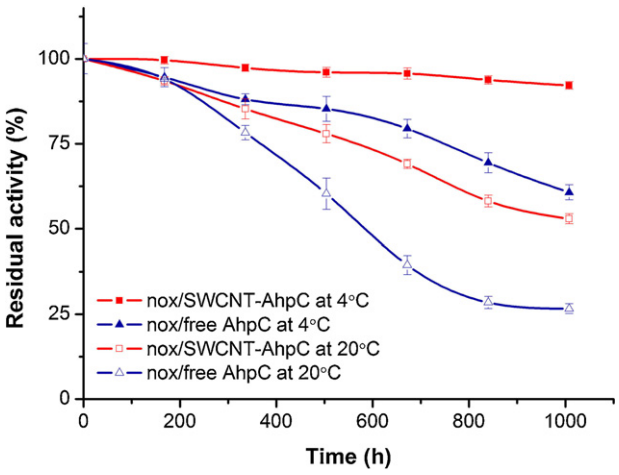

Fig. 6. Storage stability of AhpR when nox/AhpC ratio is 1:1. Nox/AhpC at 4 °C (▲), nox/AhpC at 20 °C (△), nox/SWCNT–AhpC at 4 °C (■), and nox/SWCNT–AhpC at 20 °C (□).

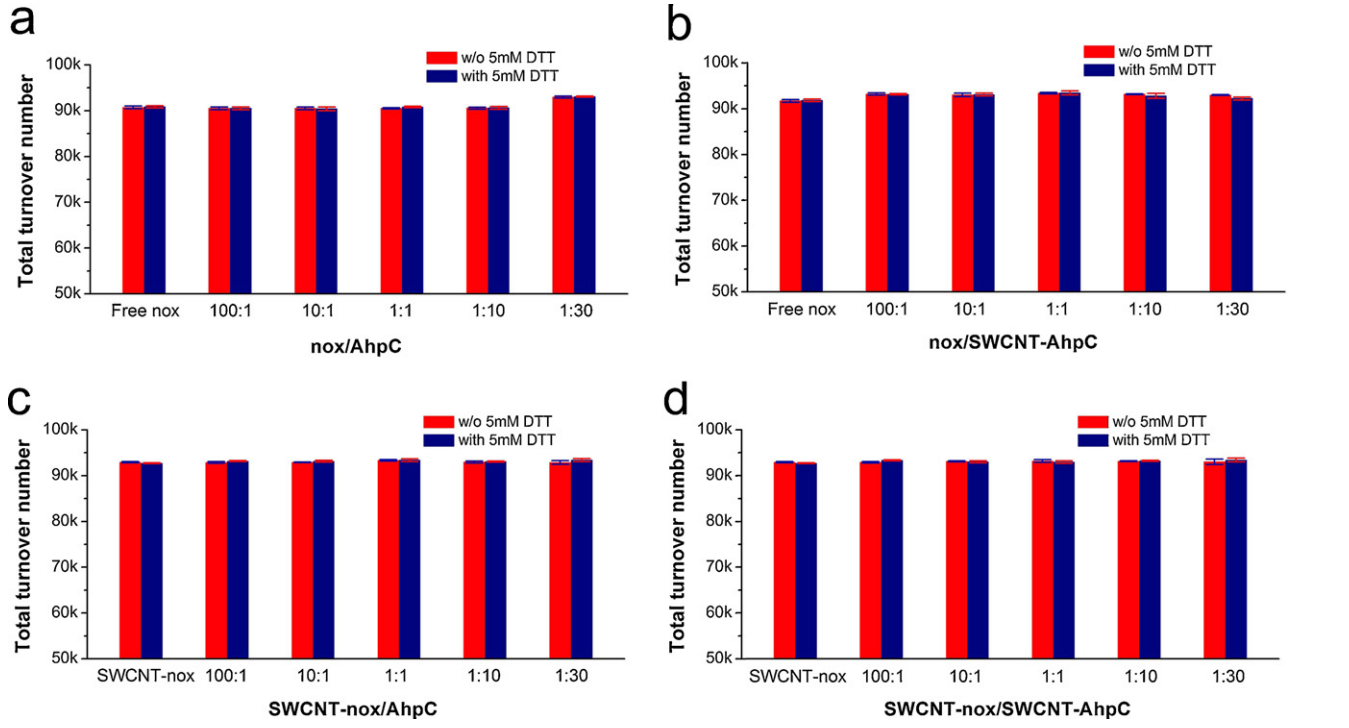

Fig. 7. Total turnover number of both free and immobilized AhpR at various nox/AhpC ratios in the presence (blue) or absence of DTT (red). (a) nox/AhpC (b) nox/SWCNT–AhpC (c) SWCNT–nox/AhpC (d) SWCNT-nox/SWCNT–AhpC. (For interpretation of the references to color in this figure legend, the reader is referred to the web version of the article.)

4. Conclusions

In summary, we have demonstrated that the non-covalent immobilization approach based on the specific interaction between His-tagged enzyme and ANTA modified nanostructures can also be applied on a consecutive biocatalytic reaction system, such as AhpR. Compared to other enzyme immobilization methods, this immobilization approach does not require enzyme purification, in another word, the cell lysate can be directly used for immobilization. Moreover, enzymes tend to have high activity retention after immobilization since the enzyme 3D structure is often well preserved via this non-covalent yet specific approach. Here, the immobilized AhpR system has shown satisfactory activity retention and improved storage stability. Various nox/AhpC ratios may affect the overall free/immobilized AhpR activity but not the operational stability, as indicated by TTN. As for the generation of intermediate hydrogen peroxide, either free or immobilized AhpC need to be present in vast excess of nox in order to act as an effective scavenger.

Acknowledgement

This work was supported by Nanyang Technological University, Singapore (Ref. SUG44/06 and RG124/06).

References

[1] A. Liese, M. Villela, Curr. Opin. Biotechnol. 10 (1999) 595–603.
[2] A. Zaks, Curr. Opin. Chem. Biol. 5 (2001) 130–136.
[3] Y.L. Li, J.H. Xu, Y. Xu, J. Mol. Catal. B-Enzym. 64 (2010) 48–52.
[4] J.H. Tao, J.H. Xu, Curr. Opin. Chem. Biol. 13 (2009) 43–50.
[5] Q.Y. Sun, Y.J. Jiang, Z.Y. Jiang, L. Zhang, X.H. Sun, J. Li, Ind. Eng. Chem. Res. 48 (2009) 4210–4215.
[6] V.M. Balcao, C. Mateo, R. Fernandez-Lafuente, F.X. Malcata, J.M. Guisan, Enzyme Microb. Technol. 28 (2001) 696–704.
[7] F. Lopez-Gallego, C. Schmidt-Dannert, Curr. Opin. Chem. Biol. 14 (2010) 174–183.
[8] W.A. Duetz, J.B. van Beilen, B. Witholt, Curr. Opin. Biotechnol. 12 (2001) 419–425.
[9] P. Wang, M.V. Sergeeva, L. Lim, J.S. Dordick, Nat. Biotechnol. 15 (1997) 789–793.
[10] D. Brady, J. Jordaan, C. Simpson, A. Chetty, C. Arumugam, F.S. Moolman, BMC Biotechnol. 8 (2008).
[11] A.I. Kallenberg, F. van Rantwijk, R.A. Sheldon, Adv. Synth. Catal. 347 (2005) 905–926.
[12] H. Zhu, J. Pan, B. Hu, H.L. Yu, J.H. Xu, J. Mol. Catal. B-Enzym. 61 (2009) 174–179.
[13] J.M. Bolivar, J. Rocha-Martin, C. Mateo, F. Cava, J. Berenguer, D. Vega, R. Fernandez-Lafuente, J.M. Guisan, J. Mol. Catal. B-Enzym. 58 (2009) 158–163.
[14] A. Haouz, A. Gelosomeyer, C. Burstein, Enzyme Microb. Technol. 16 (1994) 292–297.
[15] M.C. Messia, D. Compagnone, M. Esti, G. Palleschi, Anal. Chem. 68 (1996) 360–365.
[16] Y.S. Li, Y.D. Du, T.M. Chen, X.F. Gao, Biosens. Bioelectron. 25 (2010) 1382–1388.
[17] H.Y. Liu, T.L. Ying, K. Sun, H.H. Li, D.Y. Qi, Anal. Chim. Acta 344 (1997) 187–199.
[18] B. Ei-Zahab, D. Donnelly, P. Wang, Biotechnol. Bioeng. 99 (2008) 508–514.
[19] X. Tong, B. El-Zahab, X. Zhao, Y. Liu, P. Wang, Biotechnol. Bioeng. 108 (2011) 465–469.
[20] P. Wang, Curr. Opin. Biotechnol. 17 (2006) 574–579.
[21] J. Kim, J.W. Grate, P. Wang, Chem. Eng. Sci. 61 (2006) 1017–1026.
[22] X.B. Lu, G.F. Zou, J.H. Li, J. Mater. Chem. 17 (2007) 1427–1432.
[23] H.G. Manyar, E. Gianotti, Y. Sakamoto, O. Terasaki, S. Coluccia, S. Tumbiolo, J. Phys. Chem. C 112 (2008) 18110–18116.
[24] A.M. Klibanov, Science 219 (1983) 722–727.
[25] Sarah Hudson, Jakki Cooney, Edmond Magner, Angew. Chem. Int. Ed. 47 (2008) 8582–8594.
[26] L. Wang, L. Wei, Y. Chen, R. Jiang, J. Biotechnol. 150 (2010) 57–63.
[27] L. Wang, R. Xu, Y. Chen, R.R. Jiang, J. Mol. Catal. B: Enzym. 69 (2011) 120–126.
[28] L. Wang, H. Zhang, C.-B. Ching, Y. Chen, R.R. Jiang, Appl. Microbiol. Biotechnol. (2011), doi:10.1007/s00253-00011-03699-z.
[29] C.J. Xu, K.M. Xu, H.W. Gu, X.F. Zhong, Z.H. Guo, R.K. Zheng, X.X. Zhang, B. Xu, J. Am. Chem. Soc. 126 (2004) 3392–3393.
[30] C.J. Xu, K.M. Xu, H.W. Gu, R.K. Zheng, H. Liu, X.X. Zhang, Z.H. Guo, B. Xu, J. Am. Chem. Soc. 126 (2004) 9938–9939.
[31] Y.C. Li, Y.S. Lin, P.J. Tsai, C.T. Chen, W.Y. Chen, Y.C. Chen, Anal. Chem. 79 (2007) 7519–7525.
[32] S.H. Kim, M. Jeyakumar, J.A. Katzenellenbogen, J. Am. Chem. Soc. 129 (2007) 13254–13264.
[33] J.M. Abad, S.F.L. Mertens, M. Pita, V.M. Fernandez, D.J. Schiffrin, J. Am. Chem. Soc. 127 (2005) 5689–5694.
[34] H.R. Ellis, L.B. Poole, Biochemistry 36 (1997) 13349–13356.
[35] L.B. Poole, M. Higuchi, M. Shimada, M. Li Calzi, Y. Kamio, Free Radic. Biol. Med. 28 (2000) 108–120.
[36] Y. Niimura, V. Massey, J. Biol. Chem. 271 (1996) 30459–30464.
[37] R.R. Jiang, A.S. Bommarius, Tetrahedron Asymm. 15 (2004) 2939–2944.
[38] Z.A. Wood, L.B. Poole, P.A. Karplus, Science 300 (2003) 650–653.
[39] T.J. Jonsson, H.R. Ellis, L.B. Poole, Biochemistry 46 (2007) 5709–5721.
[40] B.R. Riebel, P.R. Gibbs, W.B. Wellborn, A.S. Bommarius, Adv. Synth. Catal. 344 (2002) 1156–1168.
[41] B.R. Riebel, P.R. Gibbs, W.B. Wellborn, A.S. Bommarius, Adv. Synth. Catal. 345 (2003) 707–712.
[42] R.R. Jiang, B.R. Riebel, A.S. Bommarius, Adv. Synth. Catal. 347 (2005) 1139–1146.
[43] L.B. Poole, Biochemistry 35 (1996) 65–75.
[44] W.F. Liu, S.P. Zhang, P. Wang, J. Biotechnol. 139 (2009) 102–107.
[45] H.F. Jia, G.Y. Zhu, P. Wang, Biotechnol. Bioeng. 84 (2003) 406–414.
[46] Y. Niimura, Y. Nishiyama, D. Saito, H. Tsuji, M. Hidaka, T. Miyaji, T. Watanabe, V. Massey, J. Bacteriol. 182 (2000) 5046–5051.
[47] E. Wehtje, P. Adlercreutz, B. Mattiasson, Biotechnol. Bioeng. 41 (1993) 171–178.
[48] G.T. Lountos, R.R. Jiang, W.B. Wellborn, T.L. Thaler, A.S. Bommarius, A.M. Orville, Biochemistry 45 (2006) 9648–9659.
[49] Z.A. Wood, L.B. Poole, P.A. Karplus, Biochemistry 40 (2001) 3900–3911.
[50] L.B. Poole, P.A. Karplus, A. Claiborne, Annu. Rev. Pharmacol. Toxicol. 44 (2004) 325–347.